RESEARCH　　　　　　　　　　　　　　　　　　　　　　　**Open Access**

Synthesis and application of CNT-supported MoO$_3$-K$_2$O nanocatalyst using microemulsion technique: role of nanoparticle size on catalyst activity and selectivity in higher alcohol synthesis

Ahmad Tavasoli[*], Saba Karimi and Morteza Shoja

Abstract

Background: Alkalized MoO$_3$ nanocatalyst supported on carbon nanotubes (CNTs) is prepared using microemulsion technique. The nanocatalyst was extensively characterized by different methods, and its activity and selectivity in higher alcohol synthesis (HAS) have been assessed in a fixed bed micro-reactor. The physico-chemical properties and performance of the nanocatalyst were compared with the catalyst prepared by impregnation method.

Results: The transmission electron microscopy images showed that small Mo nanoparticles are confined inside the CNTs (1 to 5 nm) and on the outer surface of the CNTs (1 to 7 nm). Using microemulsion technique, the average MoO$_3$ particle sizes decreased from 7 to 4.8 nm, the percentage of dispersion increased from 51 to 59 and the percentage of reduction increased by 37%. Also, the chemical interactions between K-Mo-O species increased, enhancing the conditions for the formation of alcohols.

Conclusion: The percentage of CO conversion increased from 27.7% to 43.8%. The hydrocarbon selectivity decreased from 32.4% to 24.5%, and alcohol selectivity increased from 45.3% to 61.4%.

Keywords: Higher alcohols, Molybdenum, Carbon nanotubes, Microemulsion, Particle size

Background

Higher alcohol synthesis from syngas, an economically attractive method for making fuels and chemicals, is of interest due to the enhancement of petroleum price, environmental concerns, and additive for gasoline to increase octane number [1]. There are three different methods for making higher alcohols from syngas: (1) using modified catalysts for synthesis of methanol including Cu-, Zn-, and Cr-based catalysts, (2) using modified catalysts for Fisher-Tropsch synthesis including Fe-, Ni-, and Co-based catalysts, and (3) using promoted molybdenum sulfide catalysts [2-9]. Among them, molybdenum-based catalysts are more attractive due to their high activity for the water-gas shift reaction [10]. Molybdenum disulfide (MoS$_2$) catalyst mainly produces hydrocarbons, but when it is

promoted with alkali metals, it can produce alcohols from syngas [11,12]. The function of alkali metals is to reduce the hydrogenation ability of alkyl species to form alkanes and increase the sites active for the formation of alcohols [13].

Some investigations have been carried out to study the influence of catalyst physico-chemical properties on higher alcohol synthesis and to have a better understanding of the structure-sensitive effects in higher alcohol synthesis (HAS) catalysis [14-16]. A sub-category of the structure-sensitive reactions regards the dependence of both catalytic activity and selectivity on catalytic metal particle size. Microemulsion, a novel technique for catalyst preparation, enables the control of metal particle size with a narrow particle size distribution, regardless of metal content [17-20]. Briefly, a microemulsion consists of nanosized water droplets surrounded by an oil phase, which is stabilized by a surfactant [20]. The size of the metal

* Correspondence: tavassolia@khayam.ut.ac.ir
School of Chemistry, College of Science, University of Tehran, Tehran
1417614411, Iran

particles formed in water-in-oil (w/o) microemulsions is controlled by changing the micelle size (the water-to-surfactant ratio) [20]. Hayashi et al. found that the activity of a Fe/SiO$_2$ catalyst prepared by microemulsion was higher than that of the catalyst prepared by incipient wetness impregnation with the same metal loading [21]. However, it has been also shown that metal nanoparticles obtained by microemulsion techniques interact strongly with oxygen-carrying ceramic supports (such as Al$_2$O$_3$, SiO$_2$, and TiO$_2$). Such interactions lead to a decrease of the catalyst reduction efficiency [17,22,23]. Therefore, oxidic carriers impose serious limitations to the investigation of structure-sensitive effects in catalysis because of the co-existence of incompletely reduced metal phase caused by strong interaction with the oxidic carrier [17,22,24]. Specifically, nanoparticles synthesized by microemulsion are known to be more difficult to reduce on oxidic carriers. The control of particle size is another advantage for nanoparticle preparation in microemulsion system. The ratio of water to surfactant is one of the size-determining key parameters [25]. The size of the active metal particles depends on the size of the droplets in the microemulsion. The droplet size will be influenced by the water-to-surfactant ratios. An increase of this ratio at constant concentration of surfactant will increase the average diameter of the droplets. Lisiecki and Pileni reported that the size of Cu nanoparticles prepared in a system consisting of bis(2-ethylhexyl) sulfosuccinate (aerosol-OT) surfactant, cyclohexane, and water increased from 2 to 10 nm as water-to-surfactant ratios changed from 1 to 10 [26].

In our previous works, we used impregnation method to prepare the carbon nanotube-supported MoO$_3$-K$_2$O higher alcohol synthesis catalyst [27,28]. We showed that CNTs, when used as HA synthesis catalyst support, allow a better metal dispersion and control and minimize the metal-support interactions (formation of mixed compounds). In the present work, we intend to compare the proposed microemulsion technique for MoO$_3$-K$_2$O catalyst preparation with the incipient wetness impregnation method for the control of metal particle size using CNTs as catalyst support. The influences of molybdenum particle size on the catalyst physico-chemical properties, activity, and selectivity were assessed and reported.

Methods

Multiwalled CNTs (purity >95%; characteristics are shown in Table 1) were used as support for the preparation of the catalysts. Prior to catalyst preparation, the support was treated with 30% HNO$_3$ reflux at 120°C overnight, washed with distilled water several times, and dried at 120°C for 6 h.

For the preparation of the first catalyst, molybdenum and potassium particles were synthesized in a reverse microemulsion using a nonionic surfactant Triton X-100 and *n*-hexanol as the oil phase. The concentrations of molybdenum and potassium were adjusted using aqueous solutions of (NH$_4$)6Mo$_7$O$_{24}$·4H$_2$O, (Merck, Whitehouse Station, NJ, USA) and K$_2$CO$_3$ as 15 wt.% molybdenum and 8 wt.% potassium. The water-to-surfactant molar ratio (w/s) was selected as 2. After 15 min of vigorous stirring, a microemulsion was obtained. Hydrazine was added to develop nanoparticle formation in the core of the micelles by reducing the metal oxides. Then, the purified carbon nanotubes were added under stirring. Afterward, tetrahydrofurane was added dropwise (1 ml/min). The mixture was left to mature and settle slowly overnight and then decanted. The sample was filtered and washed several times with ethanol. Next, the catalyst was dried at 120°C and calcined under argon flow at 450°C for 3 h and slowly exposed to an oxygen atmosphere during the cooling step. The catalyst prepared by this procedure was signified as C$_1$.

The second catalyst, with the same metal loadings, was prepared by the incipient wetness impregnation method using aqueous solutions of (NH$_4$)$_6$Mo$_7$O$_{24}$·4H$_2$O and K$_2$CO$_3$. After the impregnation step, the catalyst was dried at 120°C and calcined at 450°C under argon flow for 3 h and slowly exposed to an oxygen atmosphere during the cooling step. The catalyst prepared by this procedure was signified as C$_2$.

ICP-OES

The metal loadings of the fresh and purified supports and the calcined catalysts were performed using Varian VISTA-MPX inductively coupled plasma-optical emission spectrometry (ICP-OES) instrument (Varian, Palo Alto, CA, USA).

BET surface area measurements/BJH pore size distributions

Surface area, pore volume, and pore average diameter of the supports and calcined catalysts were measured using an ASAP-2010 V2 Micrometrics system (Micrometric Instrument Co., Cleveland, OH, USA). The samples were degassed at 200°C for 4 h under 50-mTorr vacuums, and their Brunauer-Emmett-Teller (BET) area, pore volume, and pore diameter were determined.

X-ray diffraction

The phases and particle sizes of the crystals present in the calcined, reduced, and sulfide catalysts were analyzed by X-ray diffraction (XRD) using a Philips Analytical X-ray diffractometer (X'Pert MPD, X'Pert, PANalytical B.V., Almelo, The Netherlands) with monochromatized Co/Kα radiation, 2θ angles from 20° to 80°. The Debye-Scherer formula ($d = 0.9\lambda / \beta\cos\theta$, where β is the full width at half maximum; λ, the wavelength of X-ray; and 0.9, a constant) was applied to MoO$_3$ peaks at 2$\theta = 43.3°$ (the most intense peak for MoO$_3$), in order to calculate the average particle sizes.

Table 1 Textural properties of the fresh and purified carbon nanotubes

Sample	BET surface area (m²/g)	Total pore volume (ml/g)	Average pore diameter (Å)	% Fe
Fresh CNTs	209	0.48	91.62	0.60
Treated CNTs	253	0.59	94.12	0

Transmission electron microscopy

The morphology of the support and catalysts was studied by transmission electron microscopy (TEM). Sample specimens for TEM studies were prepared by ultrasonic dispersion of the catalysts in ethanol, and the suspensions were dropped onto a carbon-coated copper grid. TEM investigations were carried out using a Philips CM20 (100 kV) transmission electron microscope equipped with a NARON energy-dispersive spectrometer with a germanium detector.

Temperature-programmed reduction

The H_2 temperature-programmed reduction (TPR) profiles of the catalysts were performed in order to study the reducibility of the metal species in the catalysts. The calcined catalyst sample (0.05 g) was first purged in a flow of helium at 140°C to remove traces of water and gases that exist in the catalyst, and then cooled to 40°C. Then, the TPR of each sample was performed using 5% H_2 in argon stream at a flow rate of 40 ml/min at atmospheric pressure using Micromeritics TPD-TPR 2900 analyzer (Norcross, GA, USA) equipped with a thermal conductivity detector (TCD), heating at a linearly programmed rate of 10°C/min up to 850°C.

Hydrogen chemisorption

The amount of chemisorbed hydrogen was measured using the Micromeritics TPD-TPR 2900 analyzer system. The calcined catalyst (0.2 g) was first purged in a flow of argon at 140°C to remove traces of water. The temperature was then raised to 500°C at a linearly programmed rate of 10°C/min, and the catalyst was reduced for 12 h under hydrogen flow and then cooled to 40°C. Then, the flow of hydrogen was switched to argon for 30 min in order to remove the weakly adsorbed hydrogen. Afterwards, the temperature-programmed desorption (TPD) of the samples was performed by increasing the temperature of the samples, with a ramp rate of 40°C/min, to a maximum of

Table 2 Textural properties of the catalysts

Sample	BET surface area (m²/g)	Total pore volume (ml/g)	Average pore diameter (Å)
C_1	157	0.46	127
C_2	136	0.42	129

500°C under the argon flow. The temperature-programmed desorption spectrum was used to determine the molybdenum dispersion and its average crystallite size.

Results and discussion

Characterization overview

Textural properties of the fresh and purified carbon nanotubes are given in Table 1. The data indicate that in the case of acid-washed support, surface area, total pore volume, and average internal diameter of nanotubes increased significantly which will result in better dispersion of metal as well as enhancement of the catalyst activity. Table 1 also shows the Fe content for the untreated fresh CNTs and acid-treated CNTs (determined by ICP). As shown, the amount of encapsulated metals in the fresh CNTs was 0.6 wt.% which decreased to zero after acid treatment.

Results of surface area measurements for the calcined C_1 and C_2 catalysts are given in Table 2. These results show that the BET surface area of the C_1 is 157 m²/g. However, the BET surface area for the C_2 catalyst is somewhat lower (136 m²/g), which indicates some more pore blockage by metal oxide clusters in the catalyst prepared by incipient wetness impregnation method than the catalyst prepared by microemulsion method.

The elemental compositions of the calcined catalysts measured by ICP are given in Table 3. The measured contents of the prepared catalysts are found to be slightly lower compared to the targeted values. The discrepancies may be due to the dilution of Mo because of the hygroscopic nature of the Mo precursor.

Figure 1 presents the TEM image of the purified support. As shown, the treated support is comprised of an interwoven matrix of multiwalled CNTs. TEM images of C_1 catalyst made by the microemulsion preparation route is shown in Figure 2. As shown, the very small particles are dispersed mostly inside the tubes and on the outer surface of the CNT walls. In the case of C_1 catalyst, the size of particles located inside the nanotubes and the size of particles located outside the nanotubes are within the range of 1 to 5 nm and 1 to 7 nm, respectively. The TEM image of C_2 catalyst prepared by impregnation method is shown in Figure 3. This figure shows that the particles are distributed both inside and outside of the nanotube walls.

Table 3 Chemical composition of the catalysts

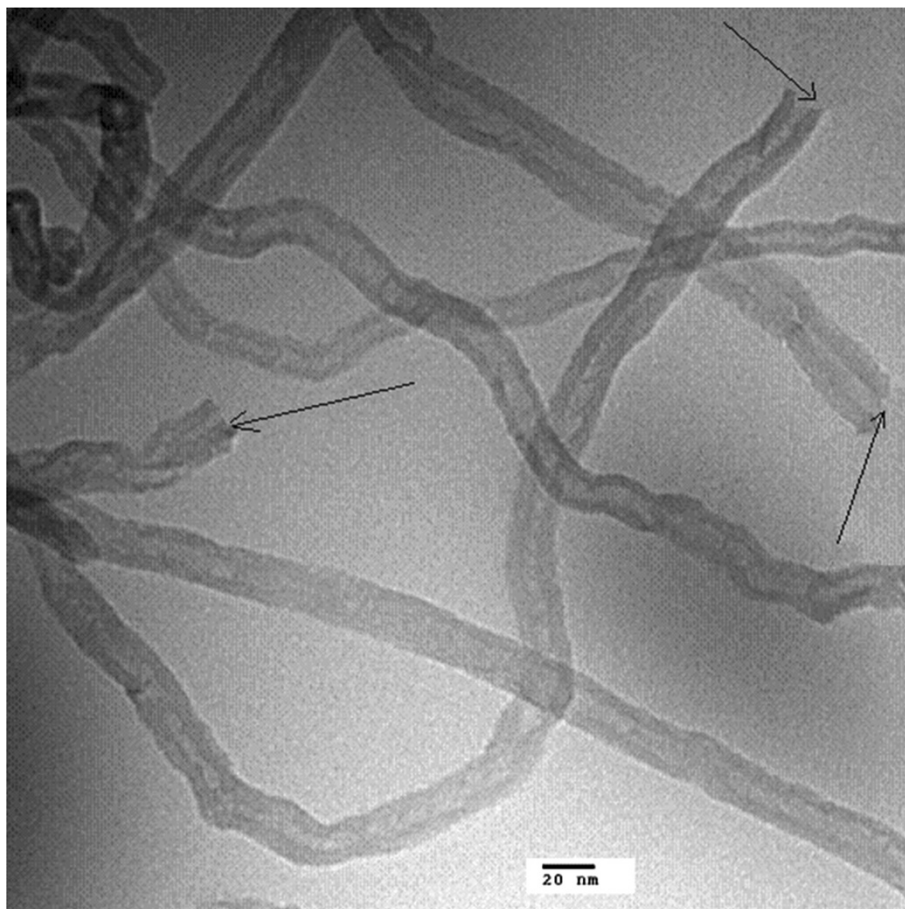| Catalyst	Targeted composition (wt.%)		Measured composition (wt.%)		Particle diameter (nm) calculated by Debye-Scherer formula
	Mo	K	Mo	K	
C_1	15	8	14.2	7.8	5.1
C_2	15	8	14.4	7.9	7.4

Figure 1 TEM image of purified CNTs. Arrows show open caps.

The size of the particles located inside the nanotubes are in the range of 3 to 9 nm. However, particles located outside the nanotubes have grown to about 16 nm. Indeed, the narrow inner diameter of the CNT channels (8 to 12 nm) restricted the insertion of particles in sizes close to the channel diameter (10 nm).

Figure 4 depicts the size distribution of the particles for C_1 and C_2 catalysts, which is determined using the population of the total particles of the catalyst based on the data taken from five TEM pictures. According to this figure, the average particle size for the C_1 and C_2 catalysts are 4.8 and 7 nm, respectively. It should be noted that using impregnation method to make the catalysts, there is no any factor to control the particle size and metal particles disperse randomly in outer and inner surfaces of the CNTs. However, using microemulsion method, the size of particles is related to the size of water droplets and the water/surfactant ratios. By controlling these parameters, it is possible to direct the size of metal particles.

To determine the crystalline phases, XRD experiments of the calcined catalysts were performed. Figure 5 presents the XRD spectrum of the catalysts with different preparation methods. To detect the phases, we used JCPDS chemical spectra data bank. As shown in this figure, using microemulsion technique decreases the intensity of the peaks corresponding to MoO_3 (peaks at 2θ values of 43.3, 63.2, and 71.9), indicating the smaller particle sizes of MoO_3 in the case of C_1 catalyst. Table 3 shows the average sizes of MoO_3 particles calculated from the XRD patterns, using the Debye-Scherer formula at 2θ value of 43.3. As can be seen, using microemulsion technique decreases the average crystal diameter of MoO_3 from 7.4 to 5.1 nm. Also, the XRD of both catalyst peaks at 2θ values of 25.8, 31.3, 40.4, and 46.3 can correspond to the crystalline structure of K-Mo-O mixed oxide species ($K_2Mo_2O_7$, K_2MoO_4, $K_2Mo_7O_{20}$, KMo_4O_6, and $K_{0.33}MoO_3$) [24-31]. In the case of C_1 catalyst, the corresponding K-Mo-O peaks appeared more significantly. This implies that using microemulsion technique, which significantly decreases the MoO_3 particle sizes, the chemical interactions between K-Mo-O species increase, enhancing the conditions for the formation of alcohols [24-31].
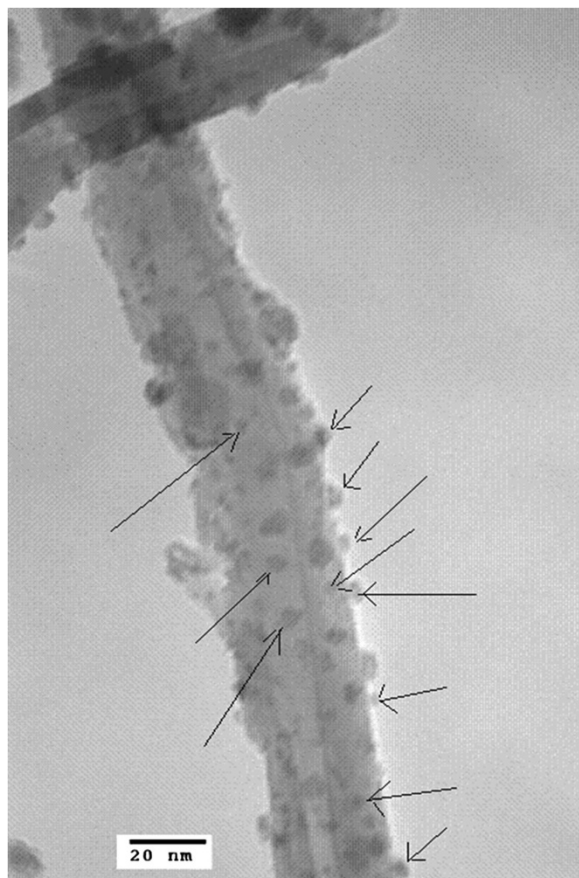
Figure 2 TEM image of the catalyst prepared by microemulsion method. Arrows show metal particles.
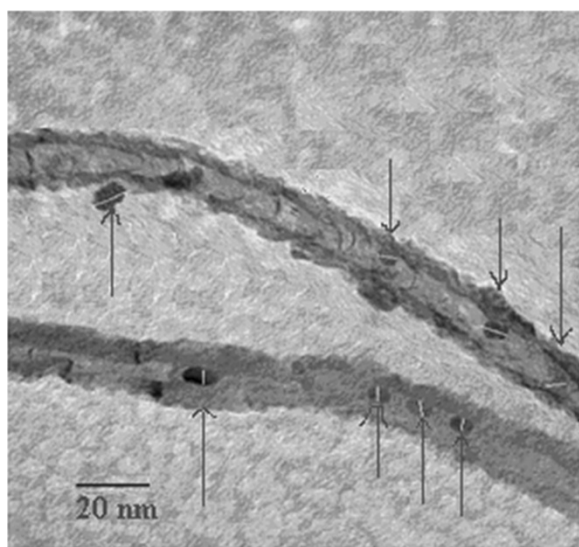

Figure 3 TEM image of the catalyst prepared by impregnation method. Arrows show metal particles.

TPR tests were performed to determine the reducibility of the calcined catalysts. The TPR spectra of the calcined C_1 and C_2 catalysts are shown in Figure 6. In the case of the catalyst prepared by impregnation method (C_2), the low temperature peak (510°C) is typically assigned to the reduction of Mo^{6+} to Mo^{4+}. The second broad peak is generally assigned to the second reduction step, which is mainly the reduction of Mo^{4+} to metallic Mo^0 [24-31]. According to Figure 6, the deposition of Mo nanoparticles synthesized by microemulsion method on the CNTs shift the reduction of the Mo^{6+} to Mo^{4+} (first peak) to a lower temperature compared to the catalyst prepared by impregnation method, indicating higher reducibility of the uniform particles. According to the TEM picture of the catalyst prepared by microemulsion technique, a good number of the small particles are located inside the tubes, which in turn lead to a better interaction with the intern electron-deficient walls of the CNTs and favor the reduction of molybdenum. The tubular morphology of the graphene layers make CNTs different compared to other carbonaceous supports. The deviation of the graphene layers from planarity causes p electron density to shift from the concave inner surface to the convex outer surface, leading to an interior electron-deficient surface and an exterior electron-enriched surface. Thus, the exterior surfaces of the CNTs are electron rich, whereas the interior ones are electron deficient, which could influence metal and metal oxide particles in contact with either surface. It can be concluded that particles located inside the carbon nanotubes are more susceptible for reduction than the particles located on the outside surfaces [24-31].

In addition, it should be noted that using microemulsion method and decreasing the particle sizes promote the formation of Mo-K mixed oxide species (as shown by XRD) that are reducible at lower temperatures. In accordance with the first TPR peak, the second peak temperature for the catalyst prepared by microemulsion method shifted to lower temperatures. The degree of catalyst reduction which is proportional to the areas of the corresponding peaks indicates that using micoemulsion technique resulted in a significant improvement in the reducibility of the catalyst (37% enhancement). In addition to the above-mentioned explanations, this can be due to the significant pore blockage for catalyst prepared by impregnation method.

The results of hydrogen chemisorption tests are given in Table 4. As shown, using microemulsion considerably increased the hydrogen uptake and percentage of dispersion. The particle diameter decreased, which is in agreement with the results of XRD and TEM tests. Higher dispersion and smaller molybdenum cluster sizes in the case of C_1 catalyst will increase the number of sites available for CO conversion and alcohol formation reaction rates.
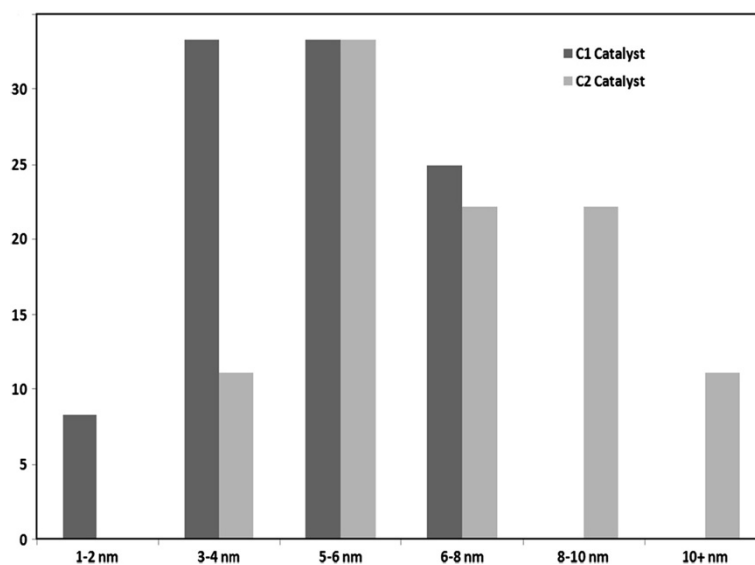
Figure 4 Particle size distribution for C_1 and C_2 catalysts.

Activity and product selectivity results

Synthesis of higher alcohols was carried out after the reduction and sulfidation of catalysts in a fixed bed reactor at 320°C, 70 bars, gas hourly space velocity of 3.6 nLit/g cat./h, and $H_2/CO = 2$. The liquid products were collected at 0°C, and the exit gas was analyzed to measure the CO conversion. The analysis of liquid products indicates that methanol and ethanol are the major products with small amounts of propanol, butanol, and other higher alcohols. The analysis of exit gas indicates that methane is the major component apart from CO, H_2, and CO_2.

Figure 7 presents the percentage of CO and H_2 conversions and different product selectivities during 24 h of continuous synthesis for C_1 and C_2 catalysts. As shown in this figure, for both catalysts, alcohols have the highest product selectivity. It has been suggested that sulfidation of the mixed oxides present in the calcined form of the catalysts and formation of the Mo-K-S species are responsible for the alcohol formation via
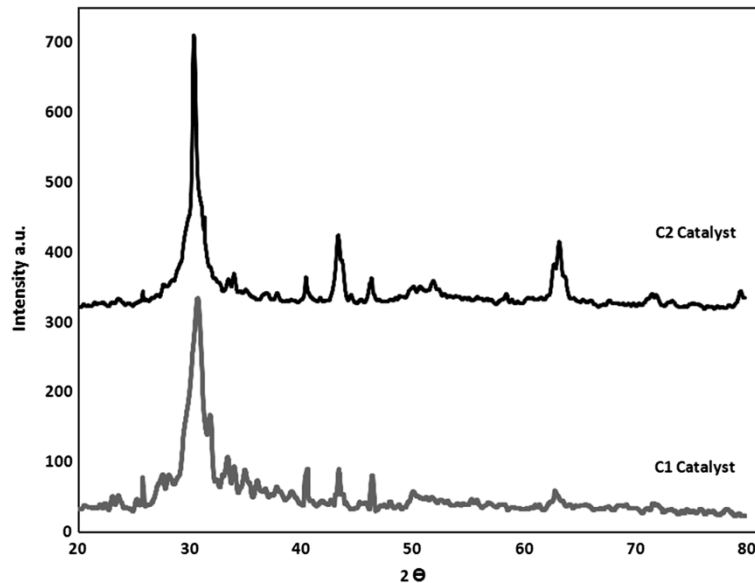

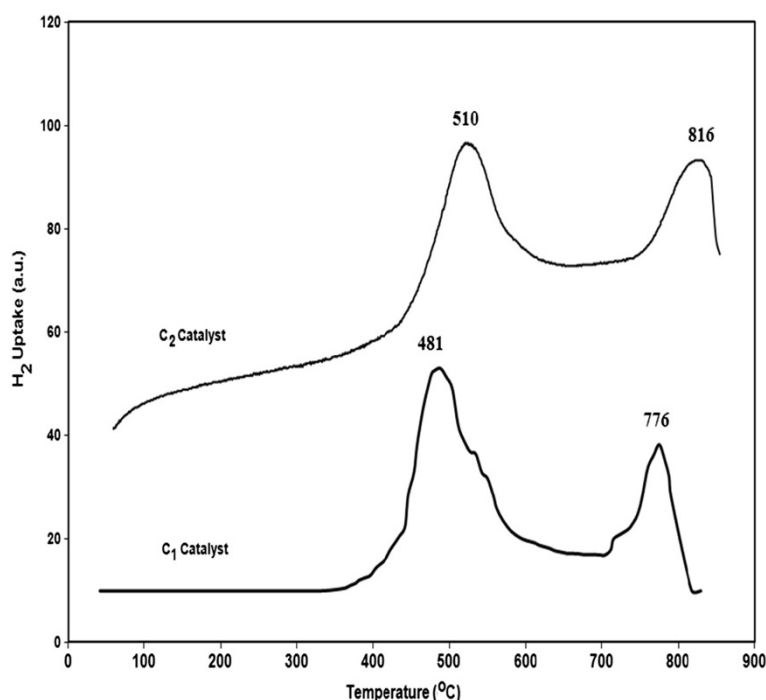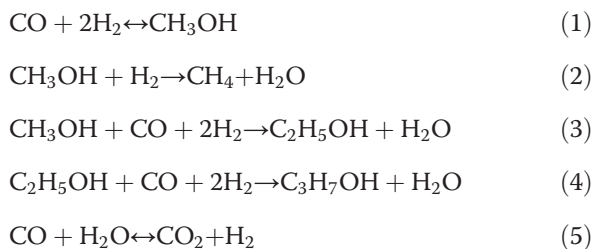**Figure 5 XRD patterns of the calcined catalysts with different preparation methods.**

Figure 6 TPR profiles for the catalysts with different preparation methods.

following CO insertion mechanism [28-31].

$$CO + 2H_2 \leftrightarrow CH_3OH \tag{1}$$

$$CH_3OH + H_2 \rightarrow CH_4 + H_2O \tag{2}$$

$$CH_3OH + CO + 2H_2 \rightarrow C_2H_5OH + H_2O \tag{3}$$

$$C_2H_5OH + CO + 2H_2 \rightarrow C_3H_7OH + H_2O \tag{4}$$

$$CO + H_2O \leftrightarrow CO_2 + H_2 \tag{5}$$

In this mechanism, adsorption of CO and hydrogen takes place at different sites to from intermediate surface species. These surface species propagate chain growth through hydrogenation, followed by insertion of molecularly adsorbed CO species to form different long-chain intermediates. The direct hydrogenation of these intermediate hydrocarbon species leads to the formation of hydrocarbon, methanol, and higher alcohols.

Figure 7 shows that using microemulsion technique for the preparation of Mo-K/CNT catalyst increases the CO and H_2 conversions significantly. The percentage of CO conversion and the percentage of H_2 conversion increased

from 27.7% to 43.8% (about 58.1% enhancement) and 23.9% to 37.6% (about 57.3% enhancement), respectively. The increase in the percentage of CO and H_2 conversions upon using microemulsion technique can be due to the increase in Mo dispersion (confirmed by XRD, TEM, and H_2 chemisorption tests) and the enhancement in reduction of Mo^{6+} to Mo^{4+} and Mo^{4+} to metallic Mo^0 (confirmed by TPR tests). Increasing dispersion, increases the number of active sites available for reaction, thus increases the activity of the catalyst [24-31].

Interestingly, Figure 7 also shows that using microemulsion technique for the preparation of Mo-K/CNT catalyst increases the selectivity of total alcohols and decreases the selectivity of hydrocarbons significantly. The total alcohol selectivity increased by 35.58%, whereas the selectivity of hydrocarbons decreased by 24.22%. Different causes can explain the significant enhancement in the selectivity of the C_1 catalyst. As shown by XRD tests, using microemulsion technique increased the chemical interactions between K-Mo-O species (the intensity of the peaks corresponding to Mo-K-O mixed oxides increased, i.e., $K_2Mo_2O_7$, K_2MoO_4, $K_2Mo_7O_{20}$, KMo_4O_6, and $K_{0.33}MoO_3$). These mixed oxides will convert to Mo-K-S species like K_2MoS_4 during catalyst reduction and sulfidation processes. The XRD patterns of the reduced and sulfurized C_1 catalyst are shown in Figure 8. As shown in Figure 8, the various diffraction peaks observed in the XRD patterns of oxide samples are completely removed after sulfidation, and the new diffraction

Table 4 H_2 chemisorption results for the catalysts

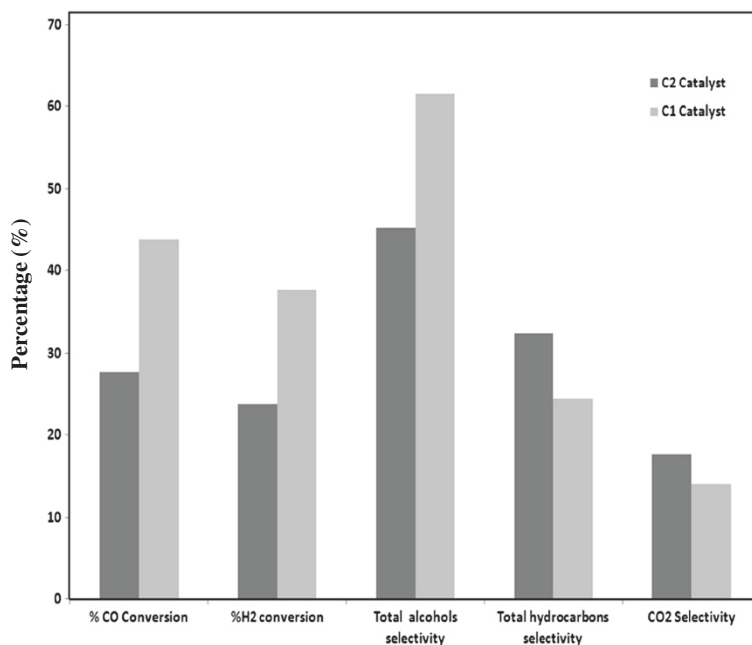| Catalyst	µmol H_2 desorbed/g cat.	% Dispersion	Particle diameter (nm)
C_1	516	59.25	4.9
C_2	399	51.1	7.1

Figure 7 Percentage of CO and H_2 conversions and different product selectivities for C_1 and C_2 catalysts.

peaks with less diffraction intensity representing different sulfide species appeared. This confirmed that newly formed active phases during the sulfidation step are well dispersed on the support. The reflections of MoS_2 crystallites are observed at 2θ values of 17.6°, 38.4°, 44.4°, and 67.9°. The peaks at 2θ values of 15.6°, 28.7° and 61.6° are due to the characteristic reflections of the K-Mo-S species, which represent KMo_3S_3.

Formation of these species can boost the conditions suitable for the formation of alcohols [24]. In addition,

the decrease in the selectivity of hydrocarbons can be due to the decreased availability of hydrogenation active centers, i.e. MoS_2 species as also confirmed by XRD results (the intensity of peaks corresponding to MoO_3 decreased in the case of C_1 catalyst).

Figure 9 shows the selectivity trends of individual alcohols for C_1 and C_2 catalysts. As shown, using microemulsion method for the preparation of Mo-K/CNT catalyst dramatically decreases the methanol selectivity and increases ethanol and other higher alcohol selectivities.
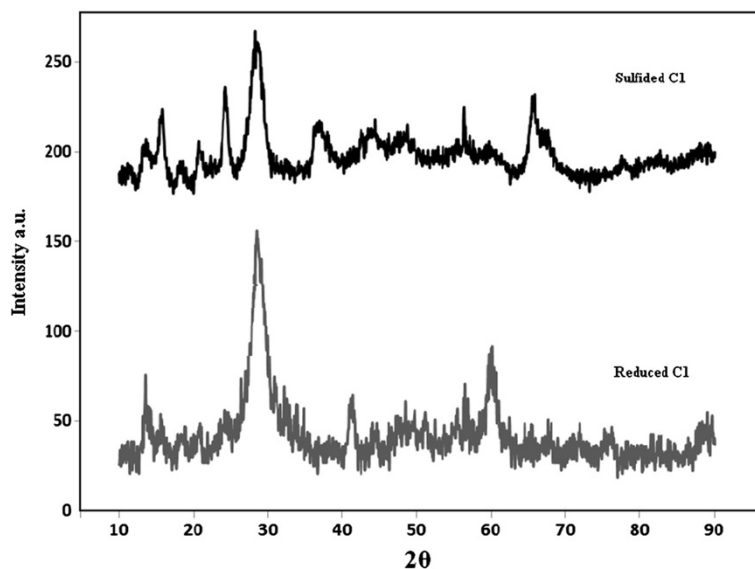

Figure 8 XRD patterns of the reduced and sulfurized C_1 catalyst.
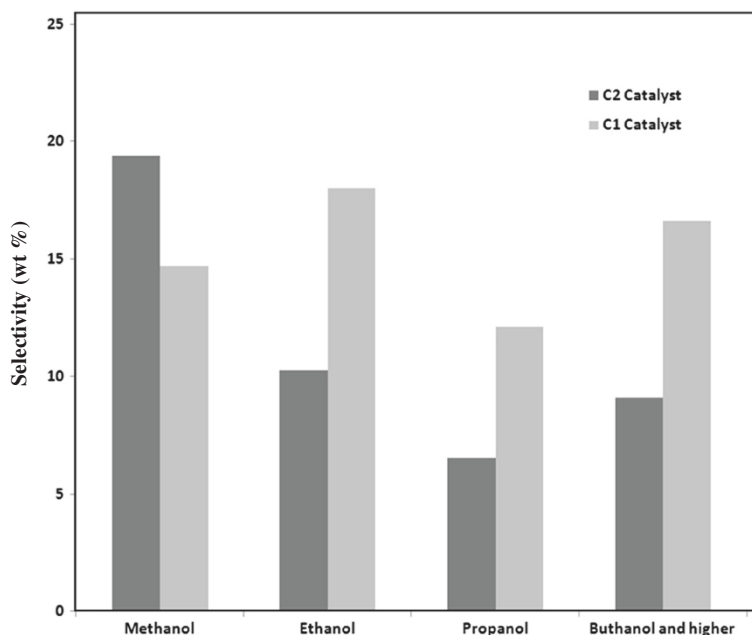
Figure 9 The selectivity trends of individual alcohols for C_1 and C_2 catalysts.

Using microemulsion technique, the methanol selectivity decreased from 19.4% to 14.7%. At the same time, the higher alcohol selectivity (C_2^+OH) increased from 25.9% to 46.7%. In an interesting research, Parmon [32] showed that a decrease in the particle size of the catalyst active phase increases the standard chemical potentials of the components and affects appreciably the adsorption equilibrium. In the case of C_1 catalyst prepared by microemulsion method, the decrease in Mo particle sizes increases the adsorption of CO and decreases the adsorption of H_2. Decreasing the amount of H_2 on the catalyst surface can suppress the formation of methane via reaction 2. Also, increasing the partial pressure of CO on the catalyst surface will express the reactions 3 and 4 which in turn increase the selectivity of ethanol and the selectivity of higher alcohols. Also, the reason may be explained from the XRD and TPD characterizations. It is clear from XRD and TPD that the C_2 catalyst showed larger MoO_3 particle size. MoO_3 will change to MoS_2 during catalyst reduction and calcination, which is responsible for poor activity of this catalyst towards the formation of higher alcohols.

Experimental
Reaction setup and experimental procedure
Higher alcohol synthesis has been performed in a tubular downflow, fixed-bed reactor system. The reactor was made up of Inconel tube of 450-mm length and 22-mm inside diameter. The reactor temperature was controlled via a PID temperature controller. Brooks 5850 mass flow controllers (Hatfield, PA, USA) were used to add H_2 and CO at the desired rate to the reactor. The reactor was packed with 0.5 g of catalyst diluted with 90-mesh-size silicon carbide and housed in a melton salt bath controlled by a temperature controller. The reactor was pressurized to 30 bars with He, and the reduction as well as the sulfurization was carried out for 6 h at 450°C at a heating rate of 2°C/min using a gas mixture containing 5 mol% H_2S in H_2 and a flow rate of 50 ml/min. The temperature was then lowered to the reaction temperature, and the system was then pressurized to the reaction condition. The feed gas mixture (H_2/CO ratio of 2) was passed through mass flow controllers, and the HAS reaction was carried out at steady state under the reaction conditions of 320°C, 70 bars, and gas hourly space velocity of 3.6 nLit/g cat./h over a period of 24 h. The product gas was cooled to 0°C and separated into gas and liquid phases at the reaction pressure. The CO, CO_2, and other gaseous products were monitored with time intervals of 1 h. The products were collected after completion of the run and analyzed by means of three gas chromatographs, a Shimadzu 4C gas chromatograph (Nakagyo-ku, Kyoto, Japan) equipped with two subsequent connected packed columns: Porapak Q and Molecular Sieve 5 Å, and a TCD with argon which was used as a carrier gas for hydrogen analysis. A Varian CP 3800 with a chromosorb column and a TCD were used for CO, CO_2, CH_4, and other non-condensable gases. A Varian CP 3800 with a Petrocol Tm DH100 fused silica capillary column and a flame ionization detector were used for liquid

products so that a complete product distribution could be provided.

Conclusions

Carbon nanotube-supported alkalized MoS_2 nanocatalysts prepared by microemulsion and impregnation methods are used to produce higher alcohols from synthesis gas. Using microemulsion technique decreased the average MoO_3 particle sizes from 7 to 4.8 nm, increased the percentage of dispersion from 51 to 59, and increased the percentage of reduction by 37%. In addition, the chemical interactions between K-Mo-O species, enhancing the conditions for the formation of alcohols, are increased. Selectivity and activity were found to be dependent on the catalyst preparation method. Using microemulsion technique increased the percentage of CO conversion from 27.7% to 43.8%. The CNT-supported MoO_3-K_2O nanocatalyst synthesized by microemulsion technique decreased the hydrocarbon selectivity from 32.4% to 24.5% and increased the alcohol selectivity from 45.3% to 61.4%. Finally, using microemulsion method for the preparation of Mo-K/CNT nanocatalyst severely decreased the methanol selectivity and increased ethanol and other higher alcohol selectivities.

References
1. Herman R (1990) Studies in surface and catalyst, Chapter 7. Elsevier, Amsterdam
2. Natta G, Colombo U, Pasquon I (131) In: Emmet PH (ed) Catalysis, vol 5. Reinhold, New York, p 131
3. Morgan GT, Hardy DVN, Procter RA (1932) J Soc Chem Ind Trans 1T:56
4. Smith, K. J.; Anderson, R. B. The Higher Alcohol Synthesis Over Promoted Cu/ZnO Catalysts. Can. J. Chem. Eng. 1983, 61, 40.
5. Smith K. J. and Anderson R. B., "A Chain Growth Scheme for the Higher Alcohols Synthesis," Journal of Catalysis, 1984, 85, 428–436.
6. Quarderer QJ, Cochram GA (1984) Catalytic process for producing mixed alcohols from hydrogen and carbon monoxide. PCT Int. Pat. Publication No. WO84/03696
7. Kinkade NE (1985) Process for producing alcohols from carbon monoxide and hydrogen using an alkali-molybdenum sulfide catalyst. PCT Int. Pat. Publication No. WO 85/03073
8. Jackson GR, Mahajan D (2001) Method for production of mixed alcohols from synthesis gas. U.S. Patent 6,248,796
9. Chaumette P, Courty P, Durand D, Grandvallet P, Travers C (1985) Process for synthesizing a mixture of primary alcohols from a synthesis gas in the presence of a catalyst containing copper, cobalt, zinc, and aluminum. GB Patent, 2,158,730
10. Woo, H. C. Park, K Y Kim, Y G Nam, I.-S.; Chung, J. S.; Lee, J. S. Mixed alcohol synthesis from carbon monoxide and dihydrogen over potassium-promoted molybdenum carbide catalysts. Appl. Catal. 1991, 75, 267-280.
11. Jiang M., Bian G.-Z., and Fu, Y.-L., "Effect of the K-Mo interaction in K-MoO3/γ-Al2O3 catalysts on the properties for alcohol synthesis from syngas," Journal of Catalysis, 1994, 146, 144–154.
12. Lee JS, Kim S, Lee KH, Nam IS, Chung JS, Kim YG, Woo HC. Role of alkali promoters in K/MoS2 catalysts for CO-H2 reactions, Volume 110, Issue 1, 1994, Pages 11–25
13. Tatsumi T., Muramatsu A., Yokota K. and Tominga H., "Mechanistic study on the alcohol synthesis over molybdenum catalysts: Addition of probe molecules to CO—H2", Jounal of Catalysis, 1989, 115, 388-398.
14. Surisetty V. R., Tavasoli A. and Dalai A. K., "Synthesis of higher alcohols from syngas over alkali promoted MoS2 catalysts supported on multi-walled carbon nanotubes," Applied Catalysis A: General, 2009, 365, 243-251.
15. Iranmahboob, J., Toghiani, H., Hill, D.O., 2003. Dispersion of alkali on the surface of Co-MoS2/clay catalyst: a comparison of K and Cs as a promoter for synthesis of alcohol. Applied Catalysis A: General, 247(2):207-218.
16. Iranmahboob J,∗. Hill DO. Alcohol synthesis from syngas over K2CO3/CoS/MoS2 on activated carbon. Catalysis Letters. 78. 1–4(2002)
17. MartŁnez A, Prieto G Breaking the dispersion-reducibility dependence in oxide-supported cobalt nanoparticles. Journal of Catalysis, 245 (2007) 245-470.
18. Kim WY, Haoka T, Kishida M, Wakabayashi K (1997) Appl Catal A 155:283
19. T. Tago; Hanaoka; T; Dhupatemiya; P; Hayashi; H; Kishida; M; Wakabayashi, K, "Effects of Rh content on catalytic behavior in CO hydrogenation with Rh-silica catalysts prepared using microemulsion", CATAL LETT, 64(1), 2000, pp. 27-31
20. Eriksson S, Nylén U, Rojas S, Boutonnet M.∗ Preparation of catalysts from microemulsions and their applications in heterogeneous catalysis, Applied Catalysis A: General 265 (2004) 207–219
21. Hayashi H, Zhe Chen L, Tago T, Kishiba M, Wakabayashi K, Catalytic properties of Fe/SiO2 catalysts prepared using microemulsion for CO hydrogenation. Applied Catalysis A: General Volume 231, Issues 1–2, 2002, Pages 81–89
22. Saib, A.M.; Claeys, M.; van Steen, E. Silica supported cobalt Fischer–Tropsch catalysts: effect of pore diameter of support. Catalysis Today vol. 71 issue 3-4, 2002. p. 395-402
23. Bezemer, G.L.; Radstake, P.B.; Koot, V.; van Dillen, A.J.; Geus, J.W.; de Jong, K.P. Preparation of Fischer-Tropsch cobalt catalysts supported on carbon nanofibers and silica using homogeneous deposition-precipitation Journal of Catalysis, Volume 237, Issue 2, 2006, Pages 291-302
24. Tavasoli A, Sadagiani K, Khorashe F, Seifkordi AA, Rohani AA, Nakhaeipour A, Cobalt Supported on Carbon nanotubes a promising Novel Fischer-Tropsch synthesis Catalyst, Fuel Process, 2006, 89 (5), 491-498
25. ZHANG X∗, ZHANG F, Synthesis of Pt–Ru–Mo ternary metal nanoparticles by microemulsions, their characterization and electrocatalytic properties, J OF Material Science 39 (2004) 5845–5848
26. Eriksson S, Nylén U, Rojas S, Boutonnet M.∗ Preparation of catalysts from microemulsions and their applications in heterogeneous catalysis, Applied Catalysis A: General 265 (2004) 207–219
27. Tavasoli A, Karimi S, Nikookar H, Molybdenum Loading Effects on the Physico-chemical Properties and Performance of Carbon Nanotubes Supported Alkalized MoS2 Catalysts for Higher Alcohols Synthesis, (2012) Iranian J of Chem & Chem Enj 31:9
28. Tavasoli A, Karimi S, Zolfaghari Z, Taghavi S, Amirfirouzkouhi H, M.A. Babatabar. Cobalt loading effects on the physico-chemical properties and performance of Co promoted alkalized MoS2/CNTs catalysts for higher alcohols synthesis
29. Surisetty V. R., Dalai, A. K. and Kozinski, J., "Intrinsic reaction kinetics of higher alcohols synthesis from synthesis gas over sulfided alkali-promoted Co-Rh-Mo trimetallic catalyst supported on MWCNTs," Energy & Fuels, 2010a, 24, 4130–4137.
30. Surisetty, V. R., Dalai, A. K., and Kozinski J., "Influence of porous characteristics of the carbon support on alkali-modified trimetallic Co–Rh–Mo sulfided catalysts for higher alcohols synthesis from synthesis gas," Applied Catalysis A: General, 2011b, 393, 50-58.

31. Surisetty V. R., Dalai A. K. and Kozinski J., "Effect of Rh promoter on MWCNT-supported alkali-modified MoS2 catalysts for higher alcohols synthesis from CO hydrogenation," Applied Catalysis A: General, 2010c, 381, 282-288.

32. Parmon VN, Thermodynamic Analysis of the Effect of the Nanoparticle Size of the Active Component on the Adsorption Equilibrium and the Rate of Heterogeneous Catalytic Processes. Physical Chemistry, 2007, 413, Part 1, pp. 42–48.